Check for updates

Post-synthetic modification of graphene quantum dots bestows enhanced biosensing and antibiofilm ability: efficiency facet†

Neha Agrawal, [ID] *[a] Dolly Bhagel, [ID] [a] Priyanka Mishra,[b] Dipti Prasad [ID] [a] and Ekta Kohli [ID] *[a]

Graphene quantum dots (GQDs) are a luminescent class of carbon nanomaterials with a graphene-like core structure, possessing quantum confinement and edge effects. They have gained importance in the biological world due to their inherent biocompatibility, good water dispersibility, excellent fluorescence and photostability. The improved properties of GQDs require the logical enactment of functional groups, which can be easily attained through post-synthetic non-covalent routes of modification. In this regard, the present work has for the first time employed a simple one-pot post-modification method utilizing the salt of amino caproic acid, an FDA approved reagent. The adsorption of the modifier on GQDs with varying weight ratios is characterized through DLS, zeta potential, Raman, absorption and fluorescence spectroscopy. A decrease of 20% in the fluorescence intensity with an increase in the modifier ratio from 1 to 1000 and an increased DLS size as well as zeta potential demonstrate the efficient modification as well as higher stability of the modified GQDs. The modified GQDs with a high weight ratio (1 : 100) of the modifier showed superior ability to sense dopamine, a neurotransmitter, as well as competent biofilm degradation ability. The modified GQDs could sense more efficiently than pristine GQDs, with a sensitivity as low as 0.06 μM (limit of detection) and 90% selectivity in the presence of other neurotransmitters. The linear relationship showed a decrease in the fluorescence intensity with increasing dopamine concentration from 0.0625 μM to 50 μM. Furthermore, the efficiency of the modified GQDs was also assessed in terms of their antibiofilm effect against *Staphylococcus aureus*. The unmodified GQDs showed only 10% disruption of the adhered bacterial colonies, while the modified GQDs (1 : 100) showed significantly more than 60% disruption of the biofilm, presenting the competency of the modified GQDs. The unique modifications of GQDs have thus proven to be an effective method for the proficient utilization of zero-dimensional carbon nanomaterials for biosensing, bioimaging, antibacterial and anti-biofilm applications.

[a]Department of Neurobiobiology, DIPAS, DRDO, New Delhi 110045, India. E-mail: neha87bhu@gmail.com; ektakohli@hotmail.com

[b]Department of Immunomodulation, DIPAS, DRDO, New Delhi-110045, India

† Electronic supplementary information (ESI) available: ESI details contains Fig. S1 (a) Uv-Visible absorption spectra of unmodified GQDs; (b) size determination of GQDs with DLS spectra; (c) fluorescence spectra of unmodified GQDs excited at 350nm (inset shows the GQDs solution in normal light and Uv light); Fig S2: pH variation of unmodified and modified GQDs; Fig. S3: Intensity ratio graph (I_0/I) with respect to dopamine concentration (a) lower concentration from 0.0625 μM to 50 μM and (b) higher concentration from 50 μM to 50 mM; Fig. S4a: Control experiment with unmodified GQDs showing no significant change at lower concentration of dopamine; Fig. S4b: Comparison of unmodified (denoted as GQDs) and modified GQDs (m1 for 1:1 modified GQDs, m3 for 1:100 modified GQDs) sensing ability for highest concentration of dopamine at 50 mM; Fig. S5: selectivity of m3GQDs system for amino acid , metal ions and neurotransmitters all at 50 μM; only dark green last epinephrine is 50 mM (where Dopamine (Dopa), Glycine (Gly), Arginine (Arg), Aspartic acid (Asp), Tyrosine (Try), Sodium ion (Na⁺), Potassium ion (K⁺), Serotonin (Sero), Epinephrine (Epi); Fig S6: Cell viability assay on C6 (Glioma) cell lines for 24 hour exposure of nanomaterials unmodified GQDs and modified (m3GQDs) GQDs; Table TS1: D and G band intensity ratio from Raman Spectra). See https://doi.org/10.1039/d2ra00494a

1. Introduction

Graphene quantum dots (GQDs), a novel class of zero-dimensional carbon nanomaterials, have gained importance in the biological world due to their biocompatible nature. Their core structure possesses graphene sheets fragmented at the quantum level to attain a three-dimensional nanoform, *i.e.* 0D.[1–3] They have an atomically thin, planar, hexagonal structure with a sp² hybridized carbon network.[4] The properties of GQDs can be modulated with respect to size, edge structure, shape, functional groups, defects, and heteroatom doping.[4] These variations during preparation give rise to surface/edge aspects and quantum confinement effects.[5,6] Properties such as tuned photoluminescence, wettability, aqueous dispersion, chemical inertness and lower cytotoxicity endow GQDs with applicability in diverse fields ranging from bioimaging[7] to photocatalysis[8] and sensors.[9]

The intrinsic fluorescence of GQDs has made them competent candidates in biosensing applications.[10,11] The sensing of

biological analytes such as antigens, physiological biomarkers, chemicals, and neurotransmitters uses the antigen–antibody reaction mechanism. Antibodies, being larger biomolecules, need to adhere to the surface of nanomaterials. This requires efficient modification to be applied during or after the synthesis of GQDs.

The top-to-bottom and bottom-to-top approaches used for the synthesis of GQDs allow many functional groups such as amine, carboxyl, epoxy, ketone, nitrogen doping, sulfur doping, and hydroxyl groups to be present on their surface.[12–16] However, the extent of functionalization and desired functional groups cannot be quantitatively measured through such methods. Post-synthetic modification is an important route of synthesis where covalent or non-covalent interactions are used for preparing desired functional group-decorated nanomaterials. Amidation,[17,18] esterification,[19,20] carbamate formation,[21] imine,[22] acid chloride,[23,24] and epoxide ring opening[25] are some covalent methods employed widely for the post-functionalization of GQDs. In comparison to covalent interactions, the non-covalent route of modification of GQDs is still in its infancy. However, non-covalent methods have expanded their significance in biological studies due to their reversible or kinetically labile nature, which enhances their importance in terms of the self-correction and preservation of the pristine structure.[26–28]

Non-covalent methods of functionalization for graphene and graphene oxide utilize polymers, biomolecules, drugs, and other carbon nano-allotropes or nanomaterials, which allow for their applications in various sectors such as energy, biosensing, and catalysis.[29] Likewise, GQD surface modification *via* the non-covalent route could be an important parameter to enhance its applicability, especially in the field of biosensing and drug delivery. Single stranded DNA (ssDNA) was adsorbed non-covalently on the GQD surface by Jeong *et al.* (2020), and they claimed a generic approach for the modification of phospholipids, peptoids and ssDNA, which could be a platform for nucleic acid sensing or for peptoid-mediated protein recognition.[28] Achadu *et al.* (2016) studied the interaction of zinc pthalocyanins with GQDs, where ZnTAPc showed covalent linkage while the other two complexes ZnTCPPc and ZnTmPyPc showed non-covalent linkage *via* π–π stacking and ionic interactions.[30] GQDs in nanocellulosic hydrogel were explored for sensing laccase *via* a non-covalent interaction between the analytes and the substrate.[31] A computational study through density functional theory (DFT) evaluated the extent of doping nitrogen in GQDs as a parameter for sensing toxic heavy metals (THMs). It was observed that the quantum theory of atoms as well as non-covalent interactions resulted in lead (Pb) having higher charge transfer and absorption energy than cadmium (Cd) and mercury (Hg).[32] Only a few experimental and theoretical works have been cited so far for the post-synthetic modification of GQDs *via* non-covalent routes for biological applications. However, the concreteness of the data and the importance of the reversible nature of non-covalent methods have inspired their wider exploration.

GQDs have also been known for their microbial functionalities. With the rise of antibiotic resistance and higher rates of infection due to biofilm formation, the antibiofilm activities of carbon nanostructures are a hot topic of study. Disruption of biofilms *via* carbon nanostructures could occur either through electrostatic or hydrophobic interactions; through the generation of reactive oxygen species as well as through interfering with self-assembled amyloid peptides.[33–35] Another major aspect of carbon nanostructures toward microbial cytotoxicity is structural defect generation in nanomaterials to enhance their bactericidal effect. Non-covalent interactions of modifiers on the surface of carbon nanostructures produce many such defects, which could play a role in antibiofilm activity. The mechanism behind graphene nanosheets of different sizes was compared in terms of antimicrobial activity, where large sheets wrapped around bacterial cells and made them starve while small sheets were more efficient as they caused oxidative stress, which arose due to intrinsic defects around the edges of the sp^2 domain and dangling bonds.[36]

The presence of heteroatoms such as in nitrogen functionalization or doping adds electron-donating atoms to the carbon structures, which facilitates electron transfer and reactive oxygen species generation, resulting in higher antibacterial ability.[37] Likewise, the effects of the oxygen moiety present in the form of ketones or carboxylic acids have also been shown to increase the antimicrobial effect. The phototoxicity of graphene oxide quantum dots toward bacteria was found to decrease the production of reactive oxygen species when the oxygen moieties were derivatized.[38] Generally, the generation of such defect sites on the GQD surface can be achieved through the photooxidation of oxygen-containing functional groups[38,39] and can be quantified through Raman and XPS techniques.[40] However, there are also other efficient methods of generating defects on carbon nanostructures, which could be beneficial towards their bactericidal properties. These make it an interesting and significant topic for the systematic study of defect generation and its role not only in antibacterial activity but also for antibiofilm applications. In this view, the present work has for the first time tried to find defect generation through the post-synthesis modification method on the GQD surface and evaluated its effect on biofilm disruption.

Thus, overall, this work is focused on modifying GQDs *via* the non-covalent route using a biocompatible modifier that can generate effective defect sites. The utilization of a non-covalent modification route through a less explored molecule such as the lithium salt of 6-aminohexanoic acid (caproic acid), an efficient modifier utilised for graphene and carbon nanotube[45] dispersions, is extended to its nanoscale counterpart GQDs, and its efficiency in biosensing as well as microbiological application was evaluated. The adsorption of such a modifier changes the pH and charge of the nanomaterials, which could eventually enhance GQD sensing as well as anti-biofilm activity. This ability of the modified GQDs was evaluated by sensing the neurotransmitter dopamine and its ability to disrupt *Staphylococcus aureus* biofilms.

2. Materials and methods

2.1 Materials

Graphene quantum dot powders were purchased from Sigma Aldrich 900726 (Product Code 1003127066). 6-Aminohexanoic

acid (AHA) was used as received from Sigma Aldrich 07260, M_w 132.18; purity: 98%. Lithium hydroxide was purchased from Sisco Research Laboratories, India, purity 98% to obtain the lithium salt of AHA (Li-AHA). The dopamine hydrochloride used was H8502-5g Cas no. 62-31-7 from Sigma Aldrich, Germany. All other chemicals were purchased from Sigma Aldrich and were utilized as obtained without any purification.

The spectrophotometer utilized for UV absorption and fluorescence study was a multimode spectrometer SYNERGY H1, Biotek, Serial. No. 1511310. pH measurements were performed using a pH meter (PCi Analytics, India) calibrated with pH 4.01 and 7.01 buffer solutions. Zeta potential measurements were obtained on a Delsa Nano C (Beckman Coulter). Pristine and Li-AHA-modified GQDs were analyzed by Raman spectroscopy with an HR 800 micro-Raman (HORIBA Jobin Yovon Technology, Japan). An incident laser with an excitation wavelength of 514 nm was used in the scanning range of 200 to 2000 cm^{-1}.

2.2 Experimental method

2.2.1 Preparation of the modifier. A 5 M DI water solution of 6-aminohexanoic acid (AHA) was added to a 5 M DI water solution of lithium hydroxide (LiOH). The solution was heated at 60 °C for 2 h until it became somewhat viscous and milky in nature. Heating was continued for 1 h at 80 °C. The formed precipitate was dried in a vacuum oven at 80 °C for 24 h. The precipitate was characterized through FT-IR and TGA to inspect the purity of formation of the lithium salt of 6-aminohexanoic acid (Li-AHA).

2.2.2 Preparation of the modified graphene quantum dots. The purchased GQDs were modified with an organic modifier, Li-AHA, as follows. 6-Aminohexanoic acid was neutralized with lithium hydroxide in deionized water to obtain the lithium salt of 6-aminohexanoic acid (Li-AHA). GQDs were ultrasonicated in deionized water for 20 min. To obtain the required GQDs/Li-AHA weight ratio, an appropriate amount of Li-AHA was added to the GQDs dispersion and was ultrasonicated in deionized water for 40 min. The Li-AHA-modified GQDs dispersion was dried at 80 °C, and then at 60 °C in a vacuum oven for 24 h to ensure the complete removal of water.

2.2.3 Biosensing of the neurotransmitter dopamine. For the sensing of the neurotransmitter, dopamine solutions were prepared with different concentrations in DI water and incubated with unmodified and modified GQDs in the desired amount at room temperature. The change in fluorescence intensity was recorded using a spectrometer and quantified.

2.2.4 Bacterial culture and propagation. The bacterial strains used in the study included the ATCC strains of *Staphylococcus aureus* (*S. aureus*-25923) obtained from the All India Institute of Medical Sciences (AIIMS), New Delhi, India. The bacterial strains were preserved and maintained as per the standard conditions and protocols.

2.2.5 Anti-biofilm activity. To evaluate the antibiofilm activity, overnight-grown bacterial cultures were diluted in MHB to obtain the desired concentration of 10^6 cells per ml. The culture was further transferred to a 96-well plate and left for 48 h for the growth of the adherent biofilm. These were subjected to modified GQDs, which were modified in three different weight ratios of the modifier, namely m1GQDs (1 : 1), m2GQDs (1 : 10), and m3GQDs (1 : 100), as well as unmodified GQDs, followed by incubation at 37 °C for 24 h. After incubation, the medium was discarded and the plate was washed gently 2–3 times with sterile PBS to remove the free-floating, detached bacterial cells. The cells were further fixed with 2% sodium acetate and the remaining biofilm was stained with 0.1% crystal violet solution for 20 min. The plates were washed 3–4 times with sterile water to remove excess stain. The plates were then air-dried at room temperature. After drying, 95% ethanol was added and the plate was read at 595 nm.

3. Result and discussion

3.1. Characterization of the modified graphene quantum dots

Graphene quantum dots were post-synthetically modified using a less explored modifier, the lithium salt of 6-aminohexanoic acid (LiAHA). The preparation of modified graphene quantum dots with the modifier Li-AHA has been reported here for the first time. However, the same modifier has been utilised for the modification of multiwalled carbon nanotubes and graphene.[43,44] The procedure of modification was inspired from these earlier works. With suitable alteration required for GQDs, the transformed procedure was optimized for the modification of graphene quantum dots. The GQDs were sonicated in a desired weight ratio (1 : 1, 1 : 10, 1 : 100, 1 : 1000) of the modifier for a definite period and the modified GQDs were characterized. Primarily, the modified GQDs were assessed for their absorption and fluorescence ability as post-synthetic modification mainly deteriorates their intrinsic properties. Hence, for the effective modification of GQDs, it is of utmost importance to optimize the conditions such that their intrinsic fluorescence ability (Fig. S1†) should diminish insignificantly. In this respect, various weight ratios of the modifier were tested to obtain the optimized conditions. For the modification of graphene quantum dots, we tested several concentration and weight ratio combinations, from which the best four concentrations are discussed here. These concentrations are logically implemented in an increasing order of weight ratio with a factor of 10. Due to their smaller size of approximately ∼5 nm, these quantum dots have a large surface-to-volume ratio and possess unique properties such as photoluminescence. Keeping in mind the end use of the modified quantum dots, modifications are required in such a manner that their intrinsic fluorescence ability is not diminished considerably, while there should be a desired change in their ionic atmosphere. This change in the ionic concentration was observed with a change in the pH, which was found to increase with an increase in the modifier ratio (Fig. S2†). The modifier consists of an ionizable carboxylate group and a long hydrophobic carbon tail that can change polarity close to the GQD surface. The amphiphilic ability of the modifier was hypothesized in earlier reports to form electrostatic interactions, causing the stabilization and dispersion of higher nanoforms of the carbon family.[43,44] Molecular dynamics

studies have been reported to understand the mechanism of action for a similar modifier. The study stated that the dispersion of graphene was facilitated by the adsorption of the modifier, which increased with increasing concentration of the modifier as the potential of mean force changes from short-range strong interactions to long-range repulsion at high weight ratios.[45] Adsorption occurs at the interface of graphene and water, resulting in a negative charge at their modified surface.[45] In this regard, the present work was inspired and in accordance with their findings, points out optimized conditions for the experimentation of GQDs with the modifier LiAHA. The modified GQDs were primarily analyzed for the change in the pH with increasing modifier ratio. The pH of the modified GQDs increases along with an increase in the negative zeta potential with an increase in the modifier ratio, which was in agreement with the earlier reported modification of carbon nanoforms.[43,44] The absorption peak and fluorescence intensity were found to drastically change with the highest concentration of the modifier, i.e. 1 : 1000, while all the other weight ratios showed only moderate (1 : 100) to no change (1 : 10, 1 : 1) in the fluorescence intensity of the modified GQDs, as shown in Fig. 1.

The absorption spectra exhibited a wavelength blueshift with increasing modifier concentration. The UV peak of the GQDs lies approximately 350 nm, as shown in Fig. S1,† which was shifted toward a lower wavelength with modification, revealing the n → π* transitions of the non-bonding electron of the C=O bonds.[41] The photoluminescence (PL) ability of the quantum dots arises due to the quantum confinement effect. GQDs possess higher quantum yields than their corresponding carbon quantum dots due to their layered structure and higher crystallinity. The adsorption of the modifier quenched the fluorescence ability of the GQDs, which is not due to Förster resonance energy transfer (FRET) since there is no spectral overlap between GQD emission and the LiAHA absorption peak. The quenching of the peak is administered with little bathochromic shift, which is commonly witnessed in non-covalently modified GQDs with biopolymers.[28] Additionally, the adsorption of the modifier involves an important dehydration step of the solvent, allowing them to overcome the electrostatic repulsion between the negatively charged modifier and the GQDs.[28] The dehydration process is important for the elimination of the solvation effect, which might hinder the approach of the modifier to the GQD surface.[42]
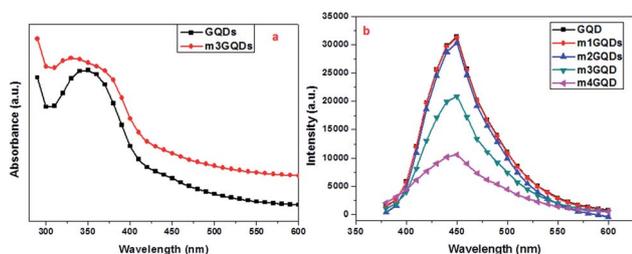
The other hypothesis proposed here is based on different studies using similar modifiers (sodium salt of aminohexanoic acid; NaAHA) for the dispersion of carbon nanotubes and graphene.[43,45] As stated earlier, one of the computational studies reveals that with the increase in modifier concentration, there exists a stronger electrostatic repulsive force than the short-range attractive force in non-covalently NaAHA-modified graphene, which allows for its better dispersion and stabilization.[45] The same concept could be hypothesized for GQDs, which when modified with LiAHA become highly stabilized and the surface passivation due to modifier adsorption could decrease the PL intensity. The extent of stabilization of the GQDs with the concentration of the modifier was quantified with the increase in the zeta potential, as shown in Fig. 2. The zeta potential highlighted a higher negative charge on the modified GQDs. The better stabilized negatively charged GQDs with higher modifier concentrations could contribute significantly to biological applications. The change in the pH, zeta potential, and the increase in the size of the GQDs with modification ascertains an efficacious non-covalent (via electrostatic force) modification process, where the modifier could adsorb on the GQD surface through amines (via hydrogen bonding) with the long hydrophobic chain outward terminated with the carboxylate ion, assembling them to obtain a negatively charged stabilized GQD structure.

The presence of the modifier on the surface of the GQDs was further demonstrated through the FT-IR spectra, as shown in Fig. 3. The peak at approximately 1647 cm^{-1} denotes the presence of the C=O of the amide or carboxylic group, while the peak around 3200 cm^{-1} was attributed to O–H stretching in the GQDs. The C=C stretching vibrations were revealed at 1500 and 3000 cm^{-1}, while the 1072 cm^{-1} peak is related to the C–O alkoxy group.[46] The FT-IR spectra of the unmodified GQDs show that the surface of the GQDs possesses hydroxyl and carbonyl groups. The modifier Li-AHA shows distinct doublet peak at approximately 1571 cm^{-1} and 1400 cm^{-1}, corresponding to carboxylate ions. The absence of the 1647 cm^{-1} peak in the modified GQDs indicates the interaction between the GQD surface and the modifier.[47] Upon modification of the GQD surface, the modified GQDs showed a shift of the peak at 1570 cm^{-1} to approximately 1590 cm^{-1} and that at 1420 cm^{-1} to 1440 cm^{-1}, which were in accordance with other studies performed with similar modifiers on graphene and the CNT surface.[44] This shift towards a higher wavenumber upon modification could be attributed to the interaction of the Li$^+$ ion of LiAHA with the pi (electron) cloud of the graphene quantum

Fig. 1 (a) UV-visible spectra of the modified GQDs (m3GQDs). (b) Fluorescence spectra of the modified GQDs excited at 350 nm (GQD: unmodified, m1GQDs: 1 : 1 modified, m2GQDs: 1 : 10 modified, m3GQDs: 1 : 100 modified, m4GQDs: 1 : 1000 modified).
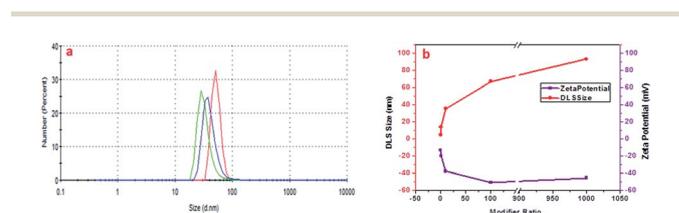

Fig. 2 (a) DLS spectra of the modified GQDs (m2GQDs, green line; m3GQDs, blue line; m4GQDs, red line). (b) Variation in DLS and zeta potential of the modified GQDs with respect to the modifier ratio.
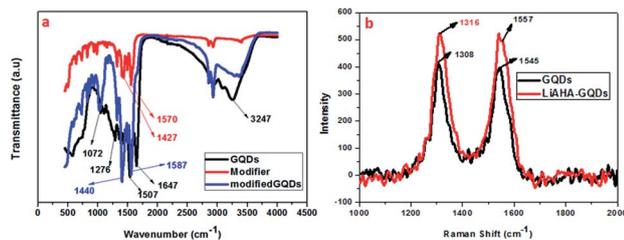
Fig. 3 : (a) FT-IR spectra of the m3GQDs, modifier, and unmodified GQDs. (b) Raman spectra of the m3GQDs.

dots, which was found to increase with increasing modifier ratio. The mode of interaction of the modifier and the GQDs could be through electrostatic attraction between the cation and the negative electron cloud, causing shifting of the peak position in the FT-IR spectrum. Raman and FT-IR are two complementary techniques that are increasingly being used for understanding the structure and functional groups on carbon nanostructures. Similar to carbon nanotubes and graphene, the GQDs also possess distinct D bands related to sp^3 hybridised carbon and G bands representing sp^2 hybridised carbon around 1318 cm^{-1} and 1660 (1595) cm^{-1}, respectively.[48] The increase in the intensity of the D and G bands is correlated with the increase in the size of the GQDs. In fact, G denotes the ordered graphitic sp^2 structure, while the defects that arise due to the modification and presence of aliphatic carbon groups on the periphery are denoted by the D band. Hence, the levels of defects generated and the degree of chemical functionalization achieved on the surface of the GQDs can be quantified by the ratio of intensity of the D and G bands.[49,50] The Raman spectra of the modified GQDs were compared with those of the unmodified GQDs, as seen in Fig. 3b. It was found that with the modification of the GQDs, there was increase in the intensity of the D and G bands. The I_D/I_G ratio of the modified GQDs was also found to be higher than that of the unmodified GQDs (Table TS1†). The increase in the size of the modified GQDs could be attributed to the adsorption of the modifier on the surface. The I_D/I_G ratio not only denotes the size but also denotes the extent of defects generated on the surface of the modified GQDs, which are higher than that on the unmodified GQDs. The shift of the Raman and IR spectra bands caused by the change in the vibrational states shows that there is a significant interaction between the modifier and the GQD surface, thus changing its surrounding atmosphere. The interaction that appears most obviously non-covalent could be supported through the increase in the size of the GQDs, as there was an increase in the intensity of the Raman and the shift of the IR bands. There could be electrostatic interactions between the ionizable cation group of the modifier and the negative charge of the GQDs. Along with this, hydrogen bonding with the already present functional moieties at the GQD surface (that arise during their synthesis) with the amine functional group of the modifier was another possibility of stabilization. Thus, the non-covalently modified GQDs possess more numerous defect sites with carboxylic acid functional groups along with the

stabilization of the dispersion, exhibiting a higher ionic dissociation ability.

3.2 Biosensing of the neurotransmitter dopamine using the modified GQDs

GQDs show excellent sensing properties against different small metal ions and biomolecules. Antioxidants such as glutathione (GSH), ascorbic acid (AA), homocysteine, and cysteine (Cys) can be sensed using hybridized forms of GQDs. GQDs adsorbed with different metal ions such as Hg^{2+}, *i.e.* GQD-Hg(II), Eu-GQD-Cu^{2+}, and GQDs-Cr(VI) have been utilized for sensing GSH, Cys, and AA respectively.[51–53] Accordingly, dopamine was polymerized and interacted with the GQDs to sense GSH.[54] Alternatively, the dopamine neurotransmitter was sensed using nitrogen-doped GQDs (NGGQDs) and the hybridized gold–nitrogen-doped GQD (Au@N-GQDs) system.[55,56] This highlights that modified GQDs can be efficiently utilized for sensing dopamine and other biological molecules.

The modified GQDs in our study were utilized for sensing the neurotransmitter dopamine. The modified GQDs (m3GQDs) showed about twofold higher sensing ability towards dopamine compared to that of unmodified GQDs. A weight ratio of 1 : 100 of the modifier (m3GQDs) was chosen as there was only a moderate change in the fluorescence spectra after modification and its pH range was found to be 9–9.5. After conducting a series of fluorescence experiments, an upgraded condition for sensing dopamine with m3GQDs was augmented. An optimized volume of 100 µl of 10 µg ml^{-1} GQDs (control) and m3GQDs (test) was used as the sensing element for 50 µl of dopamine solution in different concentration ranges, which were interacted for a duration of 30 to 45 min. All conditions for the control and test sets were kept absolutely the same and the sensing experiments were conducted at ambient temperature in the dark. A steep decrease in the fluorescence intensity resulting in nearly complete quenching was found in the range of 50 µM to 50 mM (Fig. S3b†) with modification. pH changes occurring due to modifications were monitored regularly, which were shifted towards basic pH with increasing modifier ratio (Fig. S2†). Alteration in the pH is one of the important parameters for sensing dopamine.[57] It is well known that dopamine in basic pH undergoes polymerization, which allows it to form polydopamine, which in turn can interact or form a coating around the GQDs, allowing for a significant decrease in the fluorescence intensity through Förster resonance energy transfer (FRET). The proposed hypothesis of sensing was considered as the concept behind the modifications with this particular modifier. Lower concentrations of dopamine from 0.0625 µM to 50 µM show a decrease in fluorescence intensity with increase in the concentration of dopamine, as shown in Fig. 4. The intensity ratio graph I/I_0 shows a gradual decrease in the lower concentration range of dopamine with m3GQDs (Fig. S3a†), while unmodified GQDs did not show any such distinct change in the lower range of dopamine concentration (Fig. S4a and b†), which highlights the higher sensitivity of the modified GQDs, where I and I_0 are the fluorescence intensity of m3GQDs in the presence and absence of dopamine, respectively. The linear
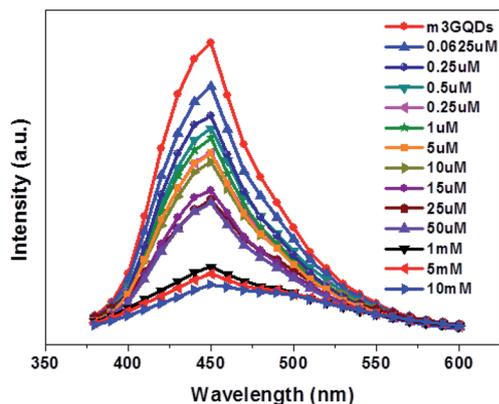
Fig. 4 (a) Fluorescence spectra of m3GQDs in the presence of dopamine.

Fig. 5 (a) Fluorescent image of m3GQDs in the presence of dopamine taken under UV lamp 360 nm; concentration from right to left to right: control to 0.0625 μM, 0.24 μM, 0.87 μM, 3.62 μM, 12.24 μM, 24 μM, 84 μM, 160 μM, and 320 μM. (b) Linear relationship curve of the I_0/I intensity ratio of the control to the test for dopamine sensing.

graph relation showed 98% regression with a detection limit of about 0.06 μM, which is much lower and competitive with previously studied fluorescent modified/hybridized GQDs.[55,56,58] Numerous systems and materials have been reported for the determination of dopamine. This novel modification of GQDs was found to be much more favorable than other systems since it is a simple one-pot step of post-synthetic modification and the sensing step did not require any heating or doping, which makes this system a versatile approach to espouse. It consumed less time, used a biocompatible material and an all-aqueous-based, was highly stable, had a well dispersed solution, and exhibited equivalent sensitivity and selectivity. The increased functional groups can make the modified GQDs highly hydrophilic, which allows them to adsorb quickly at any surface without further loss of fluorescence intensity. This faster adsorption on the surface can help in the fabrication of a paper device.

The selectivity study was conducted in the presence of other interfering amino acids such as glycine, arginine, aspartic acid, and tyrosine as well as the mineral ions sodium and potassium, which are integral parts of the blood system. The modified GQDs showed no quenching with the above-mentioned amino acids and ions, demonstrating their selectivity towards dopamine. The modified GQDs exhibit different detection performance towards the molecules glycine, arginine, aspartic acid, and tyrosine; hence, the selectivity of dopamine was determined with the modified GQDs. This change in the behaviour of the modified GQDs could be attributed to the fact that the modified GQDs possess negative charge on their surface, as determined by their zeta potential. The modified GQD 1 : 100 solutions have a pH range from 9 to 9.5. Glycine has its isoelectric point at pH 6; thus, above pH 6, it acquires negative charge. Likewise, aspartic acid and tyrosine also have negative charge. On the other hand, arginine has half negative and half positive charge at pH 9. Such a negative charge on these molecules and the negative charge on the modified GQDs could lead to repulsion between them, which could be the reason behind their inefficient detection ability towards these molecules.

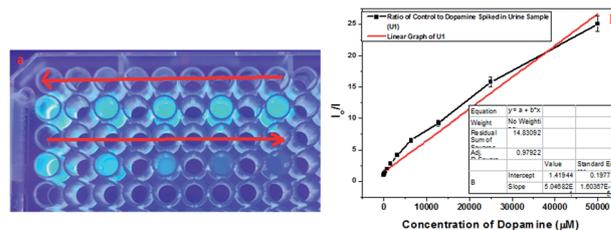Along with these, epinephrine and serotonin were also tested in the selectivity assay, in which m3GQDs were more specific towards dopamine but only interfered with epinephrine at a higher concentration, as shown in Fig. S5.† We have also evaluated dopamine monitoring in real samples by spiking a known amount of dopamine in human urine and diluting it with 1× PBS. The diluted samples were analyzed with the modified GQDs and the system works very well for determination of dopamine, as shown in Fig. 5. A linear relationship of the decrease in fluorescence intensity with an increase in dopamine concentration was observed with a regression coefficient of 97.92%. Thus, the higher specificity and selectivity of m3GQDs towards dopamine shows that the efficient modification of GQDs *via* the post-synthetic method could be a promising route for exploring the grander advantages of this zero-dimensional "rising star" of carbon nanostructure.

3.3 Antibiofilm ability of the modified GQDs

GQDs derive their properties from the graphene planar structure as well as the nano-scale size of carbon dots, making it a favorable nanoform against microbial activities. Graphene, the 'godfather' of GQDs, has excellent antimicrobial activity, whose mechanism of action is still a debated topic of research. There are many proposed hypotheses in the literature that state that oxidative stress, membrane damage, and protein dysregulation could be the cause behind their cytotoxic effects. Likewise, with regards to the mechanism of action of the antimicrobial efficacy of GQDs, only a few recent works have been cited so far.[29–31] In this regard, the present work has focused on assessing the anti-biofilm activity of modified GQDs, which are newly modified using the non-covalent post-synthesis modification route. The modified GQDs and unmodified GQDs were subjected to a cell viability study using the classical MTT (3-[4,5-dimethylthiazol-2-yl]-2,5-diphenyl tetrazolium bromide) assay on the glioma cell lines C6. The C6 cell lines were subjected to different concentrations of unmodified and modified GQDs for 24 h to observe their cell metabolic activity to find viable cells in the presence of the nanomaterials. The greater the number of viable cells, the lower the toxicity and the higher the biocompatibility of the tested nanomaterial. The unmodified and modified GQDs both showed similar viability performance with negligible cell death, showing the biocompatible nature of the unmodified and modified GQDs, as shown in Fig. S6.† The biocompatible nature of the modified GQDs (a

significant change was only observed for the highest concentration of 100 μg ml^{-1}, with the other concentrations being in an acceptable range) thus highlighted the importance of the modification method as green and versatile in terms of usage.

Staphylococcus aureus was picked as the bacterial biofilm model to study the antibiofilm activity of the modified GQDs. This species of bacteria has received special attention in medical applications due to its rising contagious infection cases owing to the growth of biofilm structures, which are also found to have antibiotic resistance. The GQDs modified with different weight ratios of the modifier, m1GQDs, m2GQDs, and m3GQDs (m4GQDs was ignored due to their significant loss of intrinsic photoluminescence ability), and unmodified GQDs were introduced to fully grown 2 day old biofilm structures (grown as per the protocol mentioned in the Experimental section) and incubated for 24 h to observe their biofilm-degradation ability. The biofilm inhibition percentage was found to increase with a higher modifier ratio of the modified GQDs; thus, the trend of biofilm inhibition was found to increase in the order of m1GQDs, m2GQDs, and m3GQDs in comparison to that of unmodified GQDs, as shown in Fig. 6. This shows that with a higher modifier ratio, the ability of GQDs to work towards biofilm degradation significantly (*p* value) increased, which could be attributed to the presence of the additional carboxylate groups in m3GQDs as compared to that in m2GQDs, m1GQDs and unmodified GQDs.

The degraded biofilm structure had a dense fully populated growth of the *S. aureus* film, which was not degraded at all in the control sample (only 15–20% degraded with unmodified GQDs, while it was most efficiently degraded to 50–60% with m3GQDs). This upsurge in the activity of the modified GQDs was found to be interesting as it opens a path for the wider applicability of competently modified GQDs. *S. aureus*, a gram-positive bacterium, possesses a thick-layered cell wall made up of peptidoglycan. In comparison, their counterparts, gram-negative bacteria, have lower contents of peptidoglycan, giving them a thin cell wall structure. However, they have a lipid bilayer lipopolysacc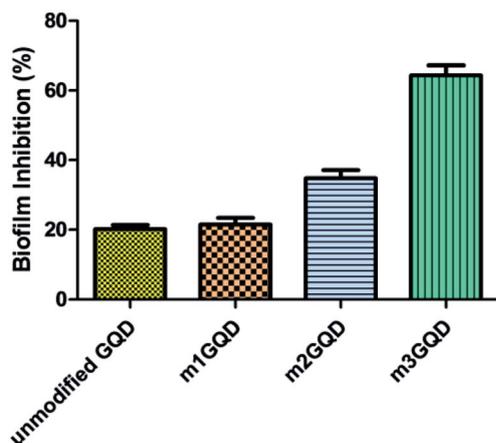haride membrane above the peptidoglycan layer and a periplasm area below it with numerous porins and appendices, making their cell wall structure remarkably strong, elastic and tough.[59]

The effect of various external stimuli such as the application of nanomaterials, antibiotics, heat, and cold plasma on the degradation of the biofilm structures of Gram-positive and Gram-negative bacteria vastly depends on their cell wall structure. In our study, we reported the biofilm growth of Gram-positive *Staphylococcus aureus* bacteria and their efficient degradation with the help of modified GQDs. The modified GQDs possess a net negative charge on their surface with an enhanced network of carboxyl and amine functional groups. Gram-positive and Gram-negative bacterial cell structures have a net negative charge. However, the content of negative charge on Gram-positive bacteria is often considered to be less than that on Gram-negative bacteria, which is still a controversial topic of study. The net charge on the surface of bacteria was determined by Ritsu *et al.*, stating that *E. coli* (gram-negative bacteria) possesses higher negative charge than *S. aureus* (gram-positive bacteria).[60] The basic differences in the cell wall structure of bacteria causes a change in their electrophoretic properties. The presence of a large amount of peptidoglycan, a glycoside linkage molecule made of NAG-NAM (*N*-acetylglucosamine coupled through a β-1,4-linkage to *N*-acetylmuramic acid), could afford preferable binding sites with the carboxyl and amine groups of the modified GQDs. In *S. aureus*, lysyl-phosphatidylglycerol is found in significant amounts.[61] This phospholipid is synthesized by a polytopic membrane protein, MprF, which catalyzes the transfer of lysine from lysyl-tRNA to phosphatidylglycerol on the inner leaflet of the membrane and then translocates this species to the outer leaflet of the membrane.[62,63] It is thought that the positive charges of lysyl-phosphatidylglycerol serve to repel positively charged antibiotics or antibiotic-metal complexes.[63,64] Since our modified GQDs possess a net negative charge, the modified GQDs could take advantage of this and cause electrostatic attraction with lysyl-phosphatidylglycerol, causing strong interactions with the cell wall and resulting in the disruption of its structure. The charge on the surface of the bacteria and the modified GQDs as well as the ionic atmosphere created due to the modified GQDs change the pH of the system towards a higher basic nature. The cell wall structure and presence of different functional groups are affected due to the differential pH gradient, which in turn can affect the degradation ability of the modified GQDs.[65] The exact mechanism of action of the modified GQDs toward gram-positive *S. aureus* needs to be studied in detail. When similar experiments were conducted for the biofilm disruption ability of GQDs towards Gram-negative *E. coli*, a lower degradation ability of the modified GQDs was observed, as shown in Fig. 7. The modified GQDs and unmodified GQDs gave nearly similar degradation effects of approximately 20–30%, which was significantly lower than that with *S. aureus*. This difference in the ability of the modified GQDs and their selectivity towards Gram-positive bacteria could be attributed to the negative charge of the modified GQDs, which could cause repulsion with the Gram-negative cell wall structure, causing less interaction and thus lower degradation occurs for these types of bacteria.
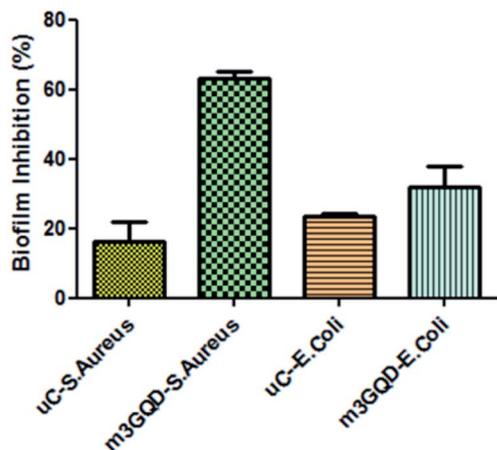

Fig. 6 Biofilm inhibition percentage of *Staphylococcus aureus* with unmodified and modified GQDs.

Fig. 7 Biofilm inhibition percentage for *S. aureus* and *E. coli* treated with m3GQDs.

Other experiments with fungal and planktonic growth are proposed as future works, where a hybrid composite of GQDs with silver nanoparticles should be applied to fight against full growth of a multispecies biofilm structure. Earlier studies on silver nanoforms have shown that positively charged silver nanoparticles (AgNPs) show efficient antimicrobial ability toward Gram-negative bacteria.[66,67] Hence, a logical combination of composite-type materials comprising modified GQDs and AgNPs could provide protection against naturally grown biofilm structures.

The mechanism behind the effective ability of the modified GQDs can be hypothesized in different ways. Our earlier discussion was based on the structure of the bacterial cell wall; the other factor could be alteration in the GQD structure due to modification. Modification adds different amounts of functional groups (*i.e.* carboxylate and amine) on the surface of the modified GQDs with respect to the ratio of the modifier. The addition of an amine group allows for the presence of the nitrogen heteroatom, which could be one of the electron-donating atoms in the carbon skeleton, aiding electron transfer and reactive oxygen species generation for the degradation of the biofilm structure.[37]

Moreover, an increase in carboxylic oxygen could add to the antimicrobial activity of the GQDs.[38,39] The modification of the GQDs allows for the generation of defect sites on their surface, which mainly happens due to distortion occurring in the structure when the modifier affects the peripheral dangling bonds and other sites, which could disorient the pristine structure. The generation of defects on the surface of the GQDs could be quantified through Raman spectroscopy by calculating the ratio of the intensity of the D to G band (I_D/I_G). As described in the characterization section, in the modified GQDs, the I_D/I_G ratio continue to increase with increasing modifier ratio, indicating higher defect site generation (Fig. 3 and Table TS1†). The higher rate of biofilm degradation for m3GQDs could thus be correlated with more numerous defect sites, which might be another reason for its oxidative stress enhancement, leading to better antibiofilm ability. However, future study needs to be

done in order to justify these proposed hypotheses, mainly for the determination of ROS in terms of functionality and defect generation to correlate it with the extent of modifier required for modification.

4. Conclusions

GQDs are extending their arms wide in the biological world, from sensing and imaging to antimicrobial activity. The development of an easy, one-pot multipurpose method for the effective modification of GQDs is thus of utmost importance in the present time. In this regard, our work has tried to focus on the formation of efficient GQDs *via* a non-covalent modification route using a novel modifier. Evaluation of the modified GQDs in terms of their biological application was assessed by their biosensing ability toward dopamine (a neurotransmitter) as well as their boosted antibiofilmcapability. The enhanced biosensing efficiency and antibiofilm ability confirm that the route of modification could be one of the versatile methods for developing GQDs, the nano-child of graphene.

Conflicts of interest

There are no conflicts to declare.

Acknowledgements

Notes and references

1 Z. Zhang, J. Zhang, N. Chen and L. Qu, Graphene quantum dots: an emerging material for energy-related applications and beyond, *Energy Environ. Sci.*, 2012, **5**, 8869.

2 J. Shen, Y. Zhu, C. Chen, X. Yang and C. Li, Facile preparation and upconversion luminescence of graphene quantum dots, *Chem. Commun.*, 2011, **47**, 2580.

3 Y. Li, Y. Zhao, H. Cheng, Y. Hu, G. Shi, L. Dai and L. Qu, Nitrogen-Doped Graphene Quantum Dots with Oxygen-Rich Functional Groups, *J. Am. Chem. Soc.*, 2012, **134**, 15.

4 M. A. Sk, A. Ananthanarayanan, L. Huang, K. H. Lim and P. Chen, Revealing the tunable photoluminescence properties of graphene quantum dots, *J. Mater. Chem. C*, 2014, **2**, 6954.

5 S. Zhu, Y. Song, J. Wang, H. Wan, Y. Zhang, Y. Ning and B. Yang, Photoluminescence mechanism in graphene quantum dots: Quantum confinement effect and surface/ edge state, *Nano Today*, 2017, **13**, 10.

6 Z. Huang, J. Qu, X. Peng, W. Liu, K. Zhang, X. Wei and J. Zhong, Quantum confinement in graphene quantum dots, *Phys. Status Solidi RRL*, 2014, **8**, 436.

7 M. K. Kumawat, M. Thakur, R. B. Gurung and R. Srivastava, Graphene Quantum Dots from *Mangifera indica*: Application in Near-Infrared Bioimaging and Intracellular Nanothermometry, *ACS Sustainable Chem. Eng.*, 2017, **5**, 1382.

8 Q. Lu, Y. Zhang and S. Liu, Graphene quantum dots enhanced photocatalytic activity of zinc porphyrin toward the degradation of methylene blue under visible-light irradiation, *J. Mater. Chem. A*, 2015, **3**, 8552.

9 F. Shi, Y. Zhang, W. Na, X. Zhang, Y. Li and X. Su, Graphene quantum dots as selective fluorescence sensor for the detection of ascorbic acid and acid phosphatase *via* Cr(vi)/ Cr(iii)-modulated redox reaction, *J. Mater. Chem. B*, 2016, **4**, 3278.

10 R. Xie, Z. Wang, W. Zhou, Y. Liu, L. Fan, Y. Li and X. Li, Graphene quantum dots as a smart probe for biosensing, *Anal. Methods*, 2016, **8**, 4001.

11 D. Bhargav, Mansuriya and Zeynep Altintas, Applications of Graphene Quantum Dots in Biomedical Sensors, *Sensors*, 2020, **20**, 1072.

12 D. Jiang, Y. Chen, N. Li, W. Li, Z. Wang, J. Zhu, H. Zhang, B. Liu and S. Xu, Synthesis of Luminescent Graphene Quantum Dots with High Quantum Yield and Their Toxicity Study, *PLoS One*, 2016, **10**, e0144906.

13 D. Yu, X. Zhang, Y. Qi, S. Ding, S. Cao, A. Zhu and G. Shi, Pb2+-modified graphene quantum dots as a fluorescent probe for biological aminothiols mediated by an inner filter effect, *Sens. Actuators, B*, 2016, **235**, 394.

14 M. Kaur, M. Kaur and V. K. Sharma, Nitrogen-doped graphene and graphene quantum dots: A review on synthesis and applications in energy, sensors and environment, *Adv. Colloid Interface Sci.*, 2018, **259**, 44.

15 W. Xuan, L. Ruiyi, F. Saiying, L. Zaijun, W. Guangli, G. Zhiguo and L. Junkang, D-penicillamine-functionalized graphene quantum dots for fluorescent detection of Fe3+ in iron supplement oral liquids, *Sens. Actuators, B*, 2017, **243**, 211.

16 X. Li, S. P. Lau, L. Tang, R. Ji and P. Yang, Sulphur doping: a facile approach to tune the electronic structure and optical properties of graphene quantum dots, *Nanoscale*, 2014, **6**, 5323.

17 Z. Luo, D. Yang, C. Yang, X. Wu, Y. Hu, Y. Zhang, L. Yuwen, E. K. L. Yeow, L. Weng, W. Huang and L. Wang, Graphene quantum dots modified with adenine for efficient two-photon bioimaging and white light-activated antibacteria, *Appl. Surf. Sci.*, 2018, **434**, 155.

18 R. V. Goreham, K. L. Schroeder, A. Holmes, S. J. Bradley and T. Nann, Demonstration of the lack of cytotoxicity of unmodified and folic acid modified graphene oxide quantum dots, and their application to fluorescence lifetime imaging of HaCaT cells, *Microchim. Acta*, 2018, **185**, 128.

19 T. Hiroyuki, N. Akihiro, F. Takanori and M. Takayuki, Molecularly designed, nitrogen-functionalized graphene quantum dots for optoelectronic devices, *Adv. Mater.*, 2016, **28**, 4632.

20 C. K. Chua, Z. Sofer, P. Šimek, O. Jankovsky, K. Klimova, S. Bakardjieva, Š. H. Kučkova and M. Pumera, Synthesis of strongly fluorescent graphene quantum dots by cage-opening buckminsterfullerene, *ACS Nano*, 2015, **9**, 2548.

21 N. R. Ko, M. Nafiujjaman, J. S. Lee, H. N. Lim, Y. k. Lee and I. K. Kwon, Graphene quantum dot-based theranostic agents for active targeting of breast cancer, *RSC Adv.*, 2017, **7**, 11420.

22 T. Hiroyuki, N. Akihiro, F. Takanori and M. Takayuki, Molecularly designed, nitrogen-functionalized graphene quantum dots for optoelectronic devices, *Adv. Mater.*, 2016, **28**, 4632.

23 M. B. Miltenburg, T. B. Schon, E. L. Kynaston, J. G. Manion and D. S. Seferos, Electrochemical polymerization of functionalized graphene quantum dots, *Chem. Mater.*, 2017, **29**, 6611.

24 A. Wolk, M. Rosenthal, S. Neuhaus, K. Huber, K. Brassat, J. K. N. Lindner, R. Grothe, G. Grundmeier, W. Bremser and R. Wilhelm, A Novel Lubricant Based on Covalent Functionalized Graphene Oxide Quantum Dots, *Sci. Rep.*, 2018, **8**, 5843.

25 D. Bhatnagar, V. Kumar, A. Kumar and I. Kaur, Graphene quantum dots FRET based sensor for early detection of heart attack in human, *Biosens. Bioelectron.*, 2016, **79**, 495.

26 M. Zheng, et al., DNA-assisted dispersion and separation of carbon nanotubes, *Nat. Mater.*, 2003, **2**, 338–342.

27 J. Zhang, et al., Molecular recognition using corona phase complexes made of synthetic polymers adsorbed on carbon nanotubes, *Nat. Nanotechnol.*, 2013, **8**, 959–968.

28 S. Jeong, R. L. Pinals, D. Bhushan, H. Song, A. Kalluri, D. Debnath, Qi Wu, M.-Ho Ham, P. Patra and M. P. Landry, Graphene Quantum Dot Oxidation Governs Noncovalent Biopolymer Adsorption, *Sci. Rep.*, 2020, **10**, 7074.

29 V. Georgakilas, J. N. Tiwari, K. Christian Kemp, J. A. Perman, A. B. Bourlinos, K. S. Kim and R. Zboril, Noncovalent Functionalization of Graphene and Graphene Oxide for Energy Materials, *Chem. Rev.*, 2016, **116**, 5464–5519.

30 O. J. Achadu, I. Uddin and T. Nyokong, Fluorescence behavior of nanoconjugates of graphene quantum dots and zinc phthalocyanines, *J. Photochem. Photobiol., A*, 2016, **317**, 12–25.

31 C. Ruiz-Palomero, S. Benítez-Martínez, M. Laura Soriano and M. Valc, Fluorescent nanocellulosic hydrogels based on graphene quantum dots for sensing laccase, *Anal. Chim. Acta*, 2017, **974**, 93–99.

32 H. R. Ghenaatian, M. Shakourian-Fard, M. R. Moghadam, G. Kamath and M. Rahmanian, Tailoring of graphene quantum dots for toxic heavy metals detection, *Appl. Phys. A: Mater. Sci. Process.*, 2019, **125**, 754.

33 H. H. Ran, X. Cheng, Y. W. Bao, X. W. Hua, G. Gao, X. Zhang, Y. W. Jiang, Y. X. Zhu and F. G. Wu, Multifunctional Quaternized Carbon Dots with Enhanced Biofilm Penetration and Eradication Efficiencies, *J. Mater. Chem. B*, 2019, **7**, 5104–5114.

34 Y. Wang, U. Kadiyala, Z. Qu, P. Elvati, C. Altheim, N. A. Kotov, A. Violi and J. S. VanEpps, Anti-Biofilm Activity of Graphene Quantum Dots via Self-Assembly with Bacterial Amyloid Proteins, *ACS Nano*, 2019, **13**, 4278–4289.

35 P. Li, S. Liu, W. Cao, G. Zhang, X. Yang, X. Gong and X. Xing, Low-Toxicity Carbon Quantum Dots Derived from Gentamicin Sulfate to Combat Antibiotic Resistance and Eradicate Mature Biofilms, *Chem. Commun.*, 2020, **56**, 2316–2319.

36 F. Perreault, A. F. de Faria, S. Nejati and M. Elimelech, Antimicrobial Properties of Graphene Oxide Nanosheets: Why Size Matters, *ACS Nano*, 2015, **9**, 7226–7236.

37 V. Strelko, V. Kuts and P. Thrower, On the Mechanism of Possible Influence of Heteroatoms of Nitrogen, Boron and Phosphorus in a Carbon Matrix on the Catalytic Activity of Carbons in Electron Transfer Reactions, *Carbon*, 2000, **38**, 1499–1503.

38 Y. Zhou, H. J. Sun, F. M. Wang, J. S. Ren and X. G. Qu, How functional groups influence the ROS generation and cytotoxicity of graphene quantum dots, *Chem. Commun.*, 2017, **53**, 10588–10591.

39 M. D. Rojas-Andrade, T. A. Nguyen, W. P. Mistler, J. Armas, J. En Lu, G. Roseman, W. R. Hollingsworth, F. Nichols, G. L. Millhauser and A. Ayzner, Chad Saltikov and Shaowei Chen; Antimicrobial activity of graphene oxide quantum dots: impacts of chemical reduction, *Nanoscale Adv.*, 2020, **2**, 1074.

40 O. Akhavan and E. Ghaderi, Toxicity of Graphene and Graphene Oxide Nanowalls Against Bacteria, *ACS Nano*, 2010, **4**, 5731–5736.

41 X. T. Zheng, A. Ananthanarayanan, K. Q. Luo and P. Chen, Glowing graphene quantum dots and carbon dots: properties, syntheses, and biological applications, *Small*, 2015, **11**, 1620.

42 S. Zheng, Q. Tu, J. J. Urban, S. Li and B. Mi, Swelling of Graphene Oxide Membranes in Aqueous Solution: Characterization of Interlayer Spacing and Insight into Water Transport Mechanisms, *ACS Nano*, 2017, **11**, 6440–6450.

43 P. V. Kodgire, A. R. Bhattacharyya, S. Bose, N. Gupta, A. R. Kulkarni and A. Misra, Control of Multiwall Carbon Nanotubes Dispersion in Polyamide6 Matrix: An assessment through Electrical Conductivity, *Chem. Phys. Lett.*, 2006, **432**, 480–485.

44 M. Sreekanth, A. S. Panwar, P. Pötschke and A. R. Bhattacharyya, Influence of hybrid nano-filler on the crystallization behaviour and interfacial interaction in polyamide 6 based hybrid nano-composites, *Phys. Chem. Chem. Phys.*, 2015, **17**, 9410–9419.

45 A. Kulkarni, N. Mukhopadhyay, A. R. Bhattacharyya and A. Singh Panwar, Dispersion of non-covalently modified graphene in aqueous medium: a molecular dynamics simulation approach, *RSC Adv.*, 2017, **7**, 4460.

46 Y. Dong, et al., Blue luminescent graphene quantum dots and graphene oxide prepared by tuning the carbonization degree of citric acid, *Carbon*, 2012, **50**, 4738–4743.

47 O. J. Achadu and I. Uddin, Tebello Nyokong Fluorescence behavior of nanoconjugates of graphene quantum dots and zinc phthalocyanines, *J. Photochem. Photobiol., A*, 2016, **317**, 12–25.

48 E. Dervishi, Z. Ji, H. Han, M. Sykora and S. K. Doorn, Raman Spectroscopy of Bottom-Up Synthesized Graphene Quantum Dots: Size and Structure Dependence, *Nanoscale*, 2019, **11**, 16571–16581.

49 Y. Shin, J. Park, D. Hyun, J. Yang and H. Lee, Generation of graphene quantum dots by the oxidative cleavage of graphene oxide using the oxone oxidant, *New J. Chem.*, 2015, **39**, 2425.

50 X. Xu, F. Gao, X. Bai, F. Liu, W. Kong and M. Li, Tuning the photoluminescence of graphene quantum dots by photochemical doping with nitrogen, *Materials*, 2017, **10**, 1328.

51 P. Yan, R. Y. Li, Y. Q. Yang, Z. J. Li, Z. G. Gu, G. L. Wang and J. K. Liu, Pentaethylene hexamine and penicillamine co-functionalized graphene quantum dots for fluorescent detection of mercury(II) and glutathione and bioimaging, *Spectrochim. Acta, Part A*, 2018, **203**, 139–146.

52 Z. Li, Y. Wang, Y. N. Ni and K. Serge, A rapid and label-free dual detection of Hg (II) and cysteine with the use of fluorescence switching of graphene quantum dots, *Sens. Actuators, B*, 2015, **207**, 490–497.

53 S. Huang, H. N. Qiu, F. W. Zhu, S. Y. Lu and Q. Xiao, Graphene quantum dots as on-off-on fluorescent probes for chromium (VI) and ascorbic acid, *Microchim. Acta*, 2015, **182**, 1723–1731.

54 S. Zhu, X. Yan, J. Qiu, J. Sun and X.-En Zhao, Turn-on fluorescent assay for antioxidants based on their inhibiting polymerization of dopamine on graphene quantum dots, *Spectrochim. Acta, Part A*, 2020, **225**, 117516.

55 X. Chen, N. Zheng, S. Chen and Q. Ma, Fluorescent Detection of Dopamine based on nitrogen-doped graphene quantum dots and visible paper based test strips, *Anal. Methods*, 2017, **9**, 2246–2251.

56 R. Dasa, K. Kumar Paula and P. K. Giria, Highly sensitive and selective label-free detection of dopamine in human serum based on nitrogen-doped graphene quantum dots decorated on Au nanoparticles: Mechanistic insights through microscopic and spectroscopic studies, *Appl. Surf. Sci.*, 2019, **490**, 318–330.

57 S. Zhu, X. Yan, J. Qiu, J. Sun and X.-En Zhao, Turn-on fluorescent assay for antioxidants based on their inhibiting polymerization of dopamine on graphene quantum dots, *Spectrochim. Acta, Part A*, 2020, **225**, 117516.

58 F. E. Lin, C. Gui, W. Wen, T. Bao, X. Zhang and S. Wang, Dopamine assay based on an aggregation-induced reversed inner filter effect of gold nanoparticles on the fluorescence of graphene quantum dots, *Talanta*, 2016, **158**, 292–298.

59 T. J. Beveridge, Structures of Gram-Negative Cell Walls and Their Derived Membrane Vesicles, *J. Bacteriol.*, 1999, 4725–4733.

60 R. Sonohara, N. Muramatsu, H. Ohshima and T. Kondo, Difference in surface properties between Escherichia coli and Staphylococcus aureus as revealed by electrophoretic

mobility measurement, *Biophys. Chem.*, 1995, **55**(3), 273–277.

61 C. M. Ernst, P. Staubitz, N. N. Mishra, S. J. Yang, G. Hornig, H. Kalbacher, A. S. Bayer, D. Kraus and A. Peschel, The bacterial defensin resistance protein MprF consists of separable domains for lipid lysinylation and antimicrobial peptide repulsion, *PLoS Pathog.*, 2009, **5**(11), e1000660.

62 S. A. Kristian, M. Dürr, J. A. Van Strijp, B. Neumeister and A. Peschel, MprF-mediated lysinylation of phospholipids in Staphylococcus aureus leads to protection against oxygen-independent neutrophil killing, *Infect. Immun.*, 2003, **71**(1), 546–549.

63 C. M. Ernst and A. Peschel, Broad-spectrum antimicrobial peptide resistance by MprF-mediated aminoacylation and flipping of phospholipids, *Mol. Microbiol.*, 2011, **80**(2), 290–299.

64 H. Nishi, H. Komatsuzawa, T. Fujiwara, N. McCallum and M. Sugai, Reduced content of lysylphosphatidylglycerol in the cytoplasmic membrane affects susceptibility to moenomycin, as well as vancomycin, gentamicin, and antimicrobial peptides, in Staphylococcus aureus, *Antimicrob. Agents Chemother.*, 2004, **48**(12), 4800–4807.

65 A. Wal, W. Norde, A. J. B. Zehnder and J. Lyklemaa, Determination of the total charge in the cell walls of Gram-positive bacteria, *Colloids Surf., B*, 1997, **9**(1–2), 81–100.

66 N. Agrawal, P. Mishra, R. Ranjan, P. Awasthi, A. Srivastava, D. Prasad and E. Kohli, Nano-cubes over nano-spheres: shape dependent study of silver nanomaterial for biological applications, *Bull. Mater. Sci.*, 2021, **44**, 191.

67 A. Abbaszadegan, Y. Ghahramani, G. Ahmad, B. Hemmateenejad, S. Dorostkar, M. Nabavizadeh and H. Sharghi, The Effect of Charge at the Surface of Silver Nanoparticles on Antimicrobial Activity against Gram-Positive and Gram-Negative Bacteria: A Preliminary Study, *J. Nanomater.*, 2015, 720654, DOI: 10.1155/2015/720654.